Research Article Open Access

Dawit Tamire Handago, Enyew Amare Zereffa*, Bedasa Abdisa Gonfa

Effects of Azadirachta Indica Leaf Extract, Capping Agents, on the Synthesis of Pure And Cu Doped ZnO-Nanoparticles: A Green Approach and Microbial Activity

https://doi.org/10.1515/chem-2019-0018
received May 22, 2018; accepted October 3, 2018.

Abstract: The current studies presented the green synthesis of zinc oxide and copper doped ZnO nanoparticles (NPs) using different ratios of Neem leaf extract and its antibacterial application on drug-resistant bacteria. The synthesized NPs were characterized using: X-ray diffractions (XRD), Fourier Transform Infrared Spectroscopy (FT-IR), Scanning Electron Microscope (SEM), UV–visible spectroscopy and a simultaneous DTA-TGA thermal analyzer. All the synthesized materials were stable above 400ºC. The powder diffraction studies indicated the formation of phase pure materials with wurtzite structure for pure ZnO and 0.5%, 1%, 1.5% Cu doped ZnO with the crystallite size in the range of 16.07 – 23.74 nm. SEM analysis revealed the formation of spherical shaped NPs with large grain size for 10% (v/v) ratio of aqueous leave extract. The aqueous extract of neem act as capping agent and prevent the NPs from agglomeration. The spectral studies confirmed the formation of NPs with the absorbance peak that is different from the micro-size ZnO. The antibacterial activities of the synthesized materials ZnO (1:1) against Staphylococcus aureus and uncalcined ZnO (7:3) and ($Zn_{0.985}Cu_{0.015}O$) against Bacillus subtilis were enhanced when referenced to the standard gentamicin.

Keywords: Nanoparticle; Wurtzite; Escherichia coli; Capping agent.

***Corresponding author: Enyew Amare Zereffa,** Department of Applied Chemistry, School of Applied Natural Science, Adama Science and Technology University, Adama, Ethiopia, E-mail: enyewama@yahoo.com
Dawit Tamire Handago, Bedasa Abdisa Gonfa: Department of Applied Chemistry, School of Applied Natural Science, Adama Science and Technology University, Adama, Ethiopia

1 Introduction

Zinc oxide NPs has been under investigations by many researchers for its medical and other applications [1, 2]. Nanoscale zinc oxide shows unique properties in comparison to its micro size. These excellent properties of ZnO NPs are due to a large number of surface zinc ions and higher surface energy, which allows increased interaction of NPs with bacteria [3]. ZnO NPs, based on its unique properties such as non- toxicity, selectivity and biocompatibility with skin, makes it a suitable additive for textiles, sunscreen emulsion, and surfaces that come in contact with human body. Therefore, it can be regarded as a promising nano-material [4]. For the synthesis of ZnO NPs, the optimization of the synthesis parameters (like temperature, precursor, time, concentration, pH of reactant, etc) leads to NPs of different size, shape, and properties. The addition of a capping molecule could also greatly influence the size confinement of nanostructures, which in turn affects the physical properties. A significant variation in size is noted with the addition of capping molecules [5-12]. The functionality and efficiency of ZnO NPs and nanostructures can be enhanced by increasing and modifying their surface by adding dopants like copper [13, 14]. For the environmental concern, researchers are using nontoxic chemicals and green methods for the synthesis of NPs for medical and other applications [15]. Several reactions require high temperature and pressure for initiation, while some require inert atmosphere protection, usage of toxic solvents, template and stabilizer for the synthesis of bioactive metal oxide NPs [16, 17]. Green approaches using microorganisms, including bacteria, fungi, yeast, and plant extracts have been used in the synthesis of NPs [17, 18]. Synthesis of NPs using microorganisms involves complicated processes due to cell cultures, and multiple purification steps. In this regard using plant extract methods for the synthesis of NPs has increasingly become a topic of interest as

Table 1: Leave extract ratios used for the synthesis of nanoparticles.

No	Precursors	Ratio of leaf extract	Abbreviation
1	$Zn(CH_3COO)_2.2H_2O$	Neem Leaf Extract (1:1) Ratio(25 mL:25mL)	ZnO(1:9)
2	$Zn(CH_3COO)_2.2H_2O$	Neem Leaf Extract (3:2) Ratio(30 mL:20mL)	ZnO(3:2)
3	$Zn(CH_3COO)_2.2H_2O$	Neem Leaf Extract (7:3) Ratio(35 mL:15mL)	ZnO(7:3)
4	$Zn(CH_3COO)_2.2H_2O$	Neem Leaf Extract (9:1) Ratio(45 mL:5mL)	ZnO(9:1)

conventional chemical methods are expensive and require the use of organic solvents as reducing and capping agents [19, 20]. In this work, we report the synthesis of pure and copper doped ZnO NPs using different ratios of Neem leaf extract in order to obtain a new product with the better antimicrobial activities [21, 22].

2 Experimental

2.1 Preparation and Characterization

Leaves of Neem (*Azadirachta Indica*) were collected and washed several times with sterilized distilled water. The aqueous extract of the sample was prepared by boiling 25 g of fresh leaves in 250 ml glass beaker along with 100 ml of double distilled water, at 60°C for 20 minutes while stirring with a magnetic stirrer until the color of the aqueous solution changed to brown. The extract was cooled to room temperature and filtered using Whatman filter paper. The extract was stored in a refrigerator to be used for the subsequent experiments [23]. To synthesize zinc oxide in (50:50) ratio 25 mL of neem leaf extract was added to 25 mL of 1M Zinc Acetate Dihydrate. The mixture was stirred continuously using magnetic stirrer and the solution was kept at pH 7.0 by dropwise addition of 0.5 M sodium hydroxide at room temperature resulted in the formation of a precipitate. The precipitate was filtered and washed repeatedly with water followed by ethanol in order to remove impurities, dried in an oven at 60°C overnight, ground to fine powder, and calcined at 400°C for 1 hour in Muffle furnace under air atmosphere. For the preparation of Cu doped ZnO ($Zn_{1-x}Cu_xO$) with: x = 0.005, 0.01 and 0.015, which are denoted as, (Cu-ZnO-05, Cu-ZnO-1 and Cu-ZnO-15), 80 mL Zn $(CH_3COO)_2.2H_2O$ (0.5033 M), 10 mL $Cu(NO_3)_2.3H_2O$ (0.02077 M) and 10 mL of neem leaf extract were mixed into 250 mL beaker. The same procedures were used with different ratios of aqueous extract as indicated in **Table 1** for the synthesis of more NPs.

2.2 Characterizations

Thermal analysis was carried out using DTA-TGA apparatus (DTG-60H, Shimadzu Co, Japan) to determine the calcination temperature of the synthesized materials. 8.475 mg of as-synthesized ZnO NPs using zinc acetate precursor and 8.117 mg of Cu doped ZnO NP samples were placed in a platinum crucible on the pan of the microbalance and heated to 1000°C, using Al_2O_3 as inert material. The phase identifications of the synthesized NPs were investigated using D8 Advance Diffractometer. XRD patterns were recorded from 2θ = 10 to 80° using CuK_α (l =1.54 Å) at 40kV, and Debye Scherrer's equation was used to estimate the crystallite size. The microstructure and surface composition of the NPs analysis were investigated with the scanning electron microscope (SEM) and Energy Dispersive X-ray Spectroscopy (EDS). The optical properties were investigated using UV–Vis spectroscopy. FTIR study was conducted on compressed pellets prepared by mixing powders with potassium bromide. Antibacterial activity of the synthesized NPs were tested against gram-positive (*Staphylococcus aureus* and *Bacillus subtilis*) and gram-negative (*Escherichia coli* and *Proteus mirabilis*) bacteria by the disc diffusion method using 200 µL of each sample with 10 mg/ml concentration saturated with 6 mm diameter disc placed on plate and incubated at 37°C for 24 hours.

Ethical approval: The conducted research is not related to either human or animal use.

3 Results and Discussion

3.1 Thermal Analysis

Figure 1 depicts the TGA-DTA curves for the thermal transformation of Zn-complex with leaf extract. TGA showed a weight loss in two steps at 110 and 400°C, while DTA showed one endothermic peak and one exothermic peak at 110 and 400°C respectively. The endothermic

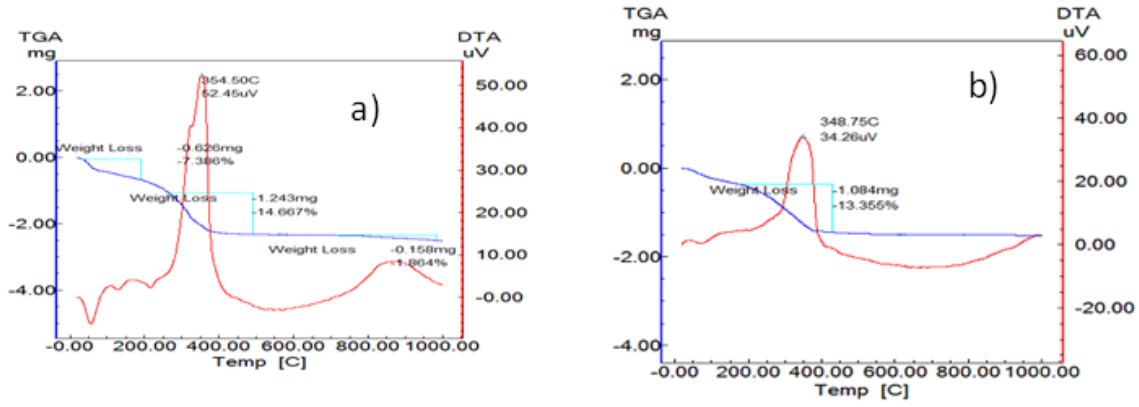

Figure 1: Thermal Analysis result of as synthesized oxides of a) ZnO and b) $Zn_{0.995}Cu_{0.005}O$.

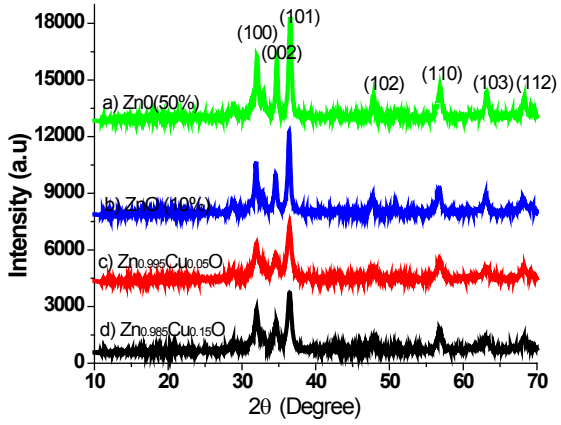

Figure 2: XRD patterns of pure ZnO synthesized using (10%, 50%) & Cu doped $Zn_{1-x}Cu_xO$ (x = 0.5% & 1.5%).

peak at 110°C was due to the removal of water and the peak at 400°C was due to decomposition of acetate ions and organic binders from leaf extracts. Dehydration from Zn-complex at 110°C is endothermic. No considerable loss was observed after 400°C up to 1000°C, which implies the ZnO and Cu-doped ZnO NPs were thermally stable above 400°C.

3.2 XRD-Analysis

Figure 2 (a, b, c & d) shows the XRD pattern of ZnO with 10%, 50% and $Zn_{1-x}Cu_xO$ samples, where: x = 0.005 and 0.015 respectively. All the indexed diffraction peaks were matched with the hexagonal phase ZnO reported in JCPDS card No 36-1451 [24, 25]. The average crystallite size of ZnO (10%), ZnO (50%), Cu doped ZnO NPs for $Zn_{0.995}Cu_{0.005}O$ and $Zn_{0.985}Cu_{0.015}O$ were found to be 19.8nm, 23.7nm, 18.4 nm, and 16.1 nm respectively.

3.3 HRSEM & EDX-Ray Spectroscopy Analysis

Figure 3(a-f), micrographs of pure and copper doped ZnONPs synthesized using different ratios of neem leaf extract revealed the influence of leaf extract or capping agent concentration on the grain size of synthesized materials.

As it is observed from SEM images of Figure 3 (b-f), the grain size of the particles increased when the volume ratios of leaf extract decreased from 50% to 10%. This is due to the high concentration of the capping agents in the reaction media. The calcinations of the as-synthesized particles removed the bonded organic capping agents and counter anions through decomposition reactions. The surface morphology of the synthesized samples viewed through the high-resolution scanning electron microscope revealed the morphology of ZnO NPs synthesized from zinc acetate has agglomerated spherical shapes. On the SEM image of Cu doped ZnO ($Zn_{0.985}Cu_{0.015}O$), Figure3c, cluster, flake-like and agglomerated spherical shapes were observed. The composition analysis of the samples determined by energy dispersive X-Ray spectroscopy (Figure 4) confirmed Zn and O are the major elements and the absence of foreign material in the spectrum.

3.4 FT-IR spectroscopy Analysis

Figure 5a-c shows the FT-IR spectra of synthesized pure & copper doped ZnO NPs using zinc acetate before and after

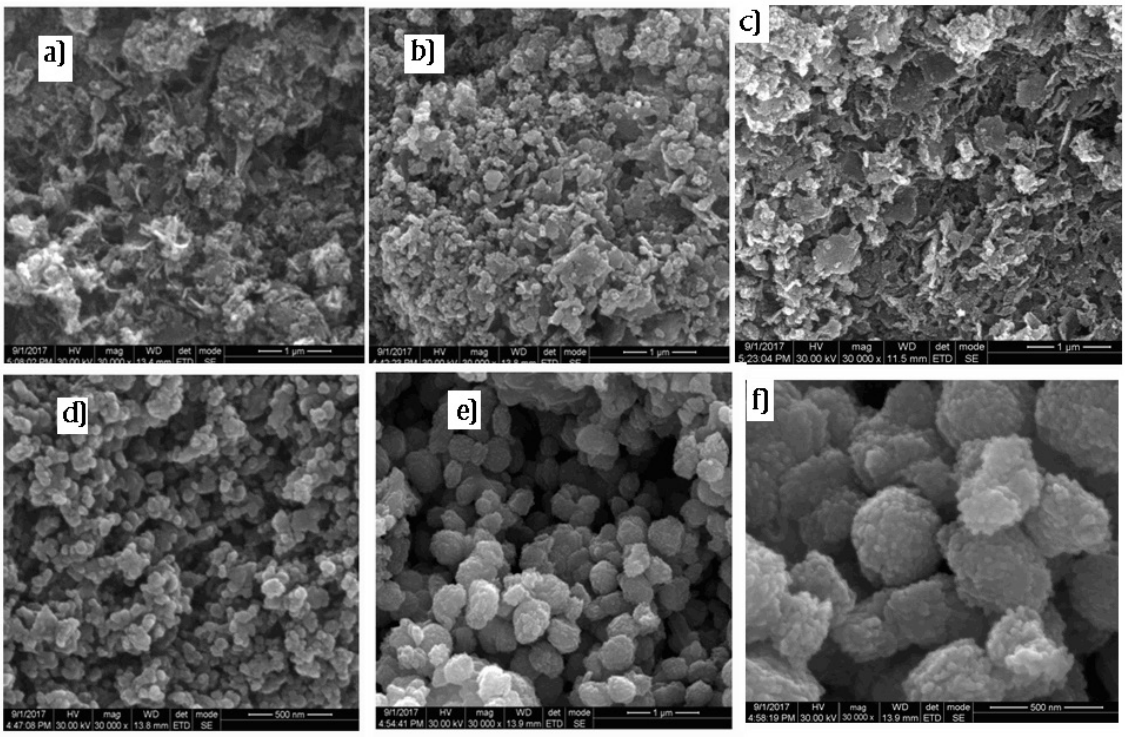

Figure 3(a-f): HRSEM micrographs of a) ZnO (1:9) not calcined, b) ZnO (1:9) calcined at 400°C, c) Cu–doped ZnO (1:9) calcined at 400°C, d) ZnO (3:2) calcined at 400°C, e) ZnO (3:7) calcined at 400°C, f) ZnO (1:1) calcined at 400°C

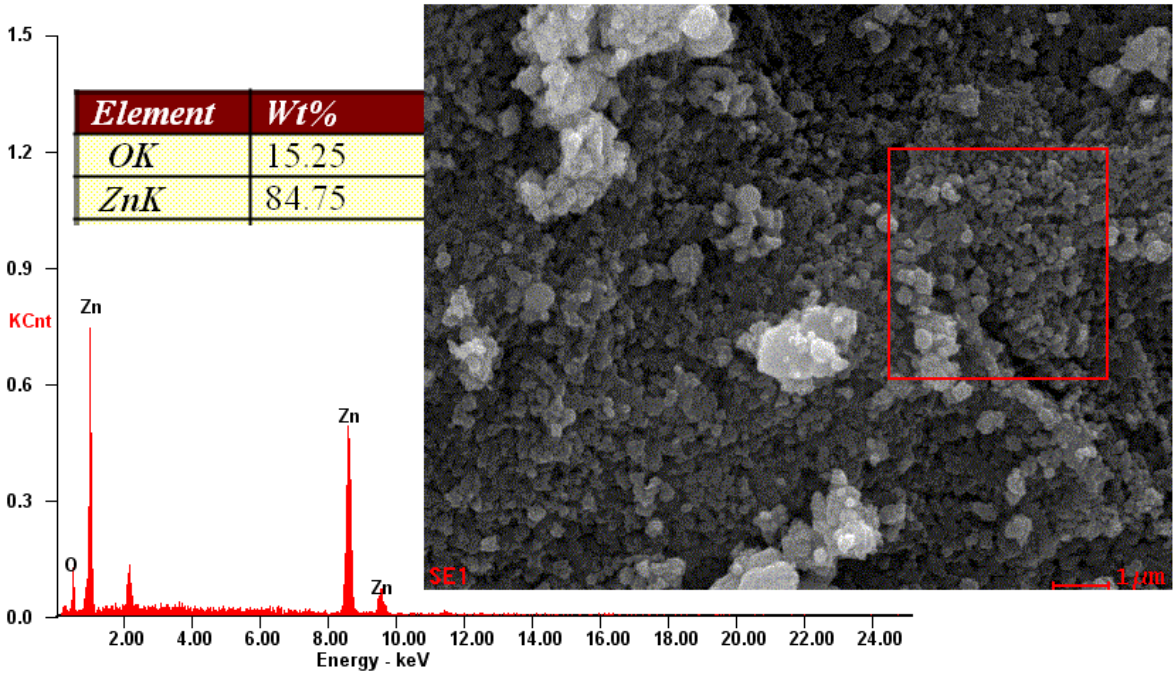

Figure 4: EDX spectrum of zinc oxide nanoparticles using zinc acetate.

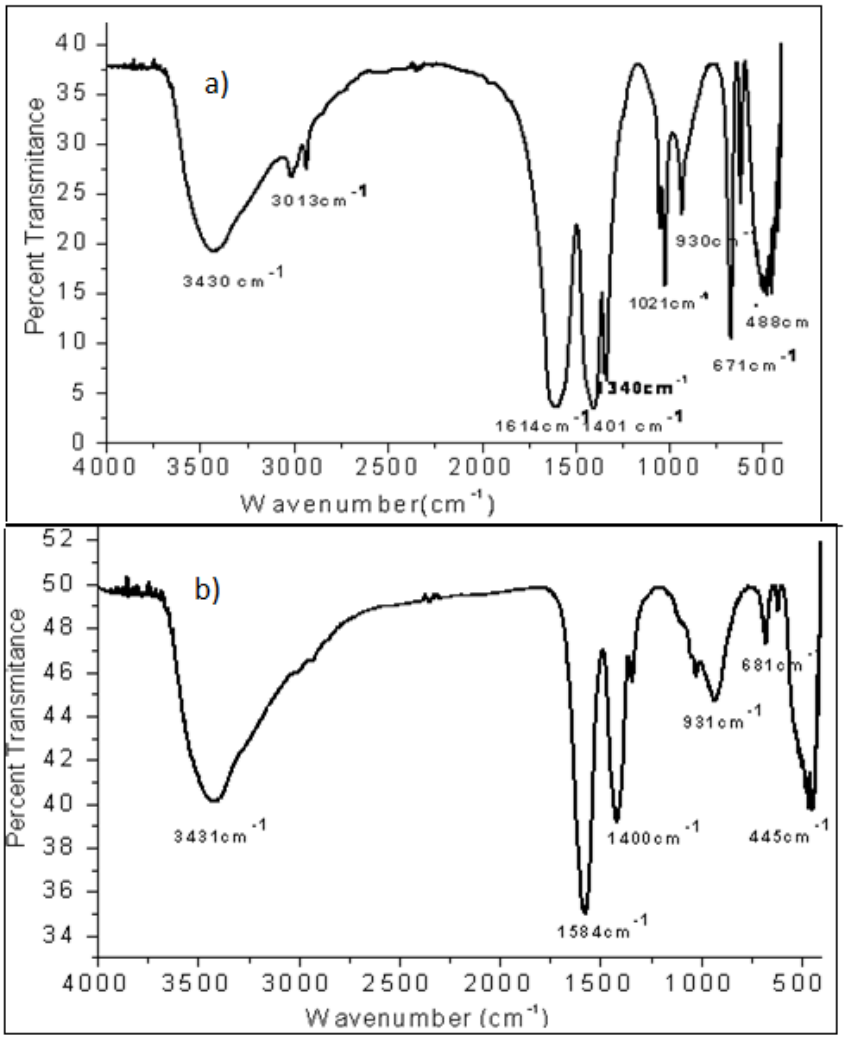

Figure 5a-b: FT-IR spectra of a) ZnO before calcinations & b) Cu doped ZnO before calcinations.

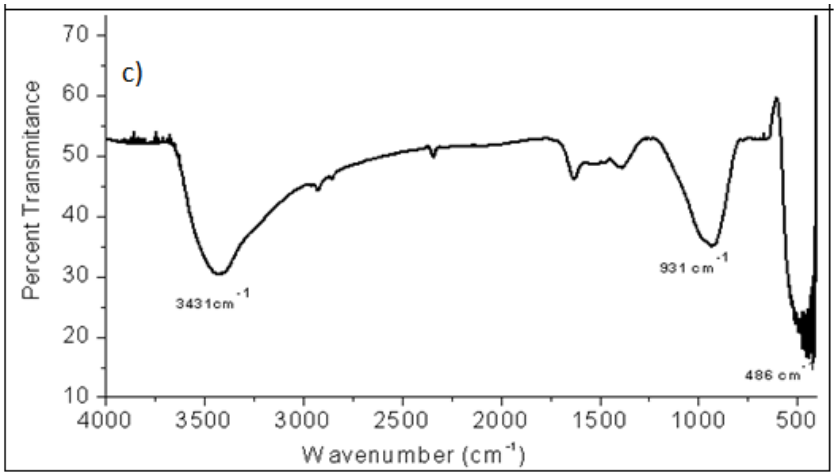

Figure 5.c: FT-IR spectra of Cu doped ZnO calcined at 400°C

Table 2: d – spacing (d_{hkl}) and Miller indices for $Zn_{1-x}Cu_xO$ (where x = 0.005 and 0.015).

For $Zn_{0.995}Cu_{0.005}O$			For $Zn_{0.985}Cu_{0.015}O$		
2θ(degree)	d – spacing (d_{hkl}) (Å)	Miller Indices h k l	2θ(degree)	d – spacing (d_{hkl}) (Å)	Miller Indices h k l
31.99	2.7953	1 0 0	31.96	2.7979	1 0 0
34.63	2.5880	0 0 2	34.60	2.5902	0 0 2
36.46	2.4622	1 0 1	36.43	2.4642	1 0 1
47.77	1.9023	1 0 2	47.74	1.9034	1 0 2
50.94	1.7911	0 0 3	50.92	1.7918	0 0 3
56.82	1.6189	1 1 0	56.80	1.6195	1 1 0
63.12	1.4717	1 0 3	63.08	1.4725	1 0 3
68.22	1.3735	1 1 2	68.20	1.3739	1 1 2

Table 3: Different angles, their corresponding FWHM values and sizes of Cu doped ZnO NPs using zinc acetate and copper nitrate precursors.

2θ(degree)	FWHM (degree)	Size of Cu doped ZnO NPs ($Zn_{0.995}Cu_{0.005}O$)(nm)	2θ(degree)	FWHM (degree)	Size of Cu doped ZnO NPs($Zn_{0.985}Cu_{0.015}O$)(nm)
31.99	0.4466	19.33	31.96	0.4417	19.53
34.63	0.4482	19.40	34.60	0.4907	17.72
36.46	0.4717	18.51	36.43	0.5512	15.84
47.77	0.5756	15.83	47.74	0.6861	12.06
50.94	0.4964	18.51	50.92	0.6507	14.05
56.82	0.5130	18.39	56.80	0.5754	16.45
63.12	0.6158	18.97	63.08	0.6313	15.45
68.22	0.5583	17.96	68.20	0.5766	17.48
Average crystallite size		**18.36**	Average crystallite size		**16.07**

calcination. The intense absorption peaks in the region 430-520 cm^{-1} correspond to the standard peak of ZnO due to ZnO stretching frequency of Zn–O bonds confirm the presence of M–O vibration bands, and the wide absorption near 3430 cm^{-1} was due to O-H stretching vibrations. The absorption occurred around 1614 cm^{-1} was due to aromatic C=C ring stretching while the strong intensity at 1401 $cm^{-1}$was due to a-CH_2 bending vibrations of aldehydes and ketones. The medium intensity around 1340 cm^{-1} was due to O-H bending. Vibrations observed around 1021 and 930 cm^{-1} were because of C-O and C-O-H stretching and bending respectively. Furthermore, **Figure 4c** indicates, the peaks intensity in 1400–1600 cm^{-1} range was relatively reduced, indicating the removal of the organic compound from the surface of ZnO NPs during calcinations. In the doped samples with copper, an absorption band near 681 cm^{-1} is also recognizable, which is related to vibration of Cu–O bond [26, 27].

3.5 UV – Visible Spectroscopy Analysis

Optical absorption spectral data of samples synthesized using (9:1, 7:3, 3:2 and 1:1) ratios of leaf extract and Cu doped $Zn_{1-x}O$ for x = 0.015 are listed in Table 4. With the increase in leaf extract ratio, the absorption curve shifted to the longer wavelengths. The red-shift result is associated with the cluster dimensions as it was confirmed on SEM micrographs.

Table 4: UV-Visible absorption spectra of Zinc oxide nanoparticles synthesized using different ratios of *neem leaf aqueous* extracts.

No	Synthesized NPs in different ratio of leave extract	l(nm)
1	ZnO (9:1)	322
2	ZnO(7:3)	368
3	ZnO (3:2)	376
4	ZnO (1:1)	386
5	($Zn_{0.985}Cu_{0.015}O$) (9:1)	376

Table 5: Zone of inhibition (mm) of ZnO NPs, Cu doped ZnO NPs and composites against gram positive and gram negative bacterial strains.

No	Bioactive agents	Zone of inhibition(mm)(Diameter)			
		Gram positive bacteria		Gram negative bacteria	
		Staphylococcus aureus	*Bacillus subtilis*	*Escherichia coli*	*Proteus mirabilis*
1	ZnO(9:1)	10 mm	6 mm	7 mm	6 mm
2	ZnO(7:3)	12 mm	6 mm	6 mm	6 mm
3	ZnO(3:2)	12 mm	6 mm	6 mm	6 mm
4	ZnO(1:1)	13 mm	6 mm	6 mm	6 mm
5	Cu-ZnO-05	10 mm	7 mm	6 mm	6 mm
6	Cu-ZnO-1	8 mm	7 mm	7 mm	6 mm
7	Cu-ZnO-15	7 mm	8 mm	8 mm	6 mm
8	*ZnO(7:3)	6 mm	15 mm	6 mm	6 mm
9	*Cu-ZnO-15	6 mm	16 mm	6 mm	6 mm
10	Gentamicin	12 mm	14 mm	14 mm	14 mm

*ZnO(7:3) & *Cu-ZnO-15 are samples without calcinations

The results in Table 5 showed the microbial activities of ZnO and copper doped ZnO NPs synthesized using leaf extract with different ratios. Zone of inhibition for Cu doped ZnO NPs increased with the concentration of dopant: $Zn_{0.995}Cu_{0.005}O$ to $Zn_{0.985}Cu_{0.015}O$ (6mm to 8mm) on *Bacillus subtilis* and decreased on *S.aureus* (from 10mm to 7mm). Also, inhibitions of 15 and 16 mm were recorded for *ZnO (7:3) and *Cu-ZnO-15. This might be due to the synergetic effect of leaf extract, ZnO and CuO NPs. The influence of the leaf extract ratios and dopant concentration were clearly observed on gram-positive, *Staphylococcus aureus* bacteria.

4 Conclusions

Pure and Cu doped zinc oxide NPs with wurtzite structures were synthesized using different ratios of neem leaf extract by the co-precipitation method. All the synthesized materials were stable above 400ºC. The microstructure investigation revealed the influence of leaf extract ratios on the morphology of the particles. The antibacterial studies of the synthesized composite materials revealed the synergetic effect of leaf extract, ZnO and CuO NPs on the gram-positive *Bacillus subtilis*.

Conflict of interest: Authors declare no conflict of interest.

References

[1] Xie Y., He Y., Irwin P. L., Jin T., Shi X., Antibacterial activity and mechanism of action of zinc oxide nanoparticles against Campylobacter jejuni, Appl. Environ. Microbiol., 2011, 77, 2325-31. http://dx.doi.org/10.1128/AEM.02149-10

[2] Joshi P., Chakraborti S., Chakrabarti P., Singh S.P., Ansari Z.A., Husain M., ZnO Nanoparticles as an Antibacterial Agent Against E. coli, Sci. Adv. Mater., 2012, 4, 173-178, http://dx.doi.org/10.1166/sam.2012.1269

[3] Jones N., Ray B., K. Ranjit T., Manna A. C., Antibacterial activity of ZnO nanoparticle suspensions on a broad spectrum of microorganisms, FEMS Microbiol. Lett., 2008, 279, 71-76. http://dx.doi.org/10.1111/j.1574-6968.2007.01012.x
[4] Zhao S.W., Guo C.R., Hu Y.Z., Guo Y.R., Pan Q.J., The preparation and antibacterial activity of cellulose/ZnO composite, Open J. Chem., 2018, 16, 9–20. https://doi.org/10.1515/chem-2018-0006
[5] Tian Z. R., Voigt J. A., Liu J., Mckenzie B., Mcdermott M. J., Biomimetic arrays of oriented helical ZnO nanorods and columns, J. Am. Chem. Soc., 2002, 124, 12954-5.https://pubs.acs.org/doi/abs/10.1021/ja0279545
[6] Zhang D., Zhang J., Wu Q., Miu X., Ultraviolet emission of ZnO nano-polycrystalline films by modified successive ionic layer adsorption and reaction technique, J. Sol-Gel Sci. Technol., 2010, 54, 165-173. https://link.springer.com/article/10.1007/s10971-010-2171-3
[7] Oliveira A.P., Hochepied J.F., Grillon F., Berger M.H., Controlled Precipitation of Zinc Oxide Particles at Room Temperature, Chem. Mater., 2003, 15, 3202–3207. https://pubs.acs.org/doi/abs/10.1021/cm0213725
[8] Kisailus D., Schwenzer B., Gomm J., Weaver J.C., Morse E., Kinetically controlled catalytic formation of zinc oxide thin films at low temperature, J. Am. Chem. Soc., 2006, 128, 10276-80, https://pubs.acs.org/doi/abs/10.1021/ja062434l
[9] Osmond M.J., McCall M.J, Zinc oxide nanoparticles in modern sunscreens: an analysis of potential exposure and hazard, Nanogk., 2010, 4, 15–41. https://doi.org/10.3109/17435390903502028
[11] Singh A.K., Viswanath V., Janu V.C., Synthesis, the effect of capping agents, structural, optical and photoluminescence properties of ZnO nanoparticles, J. Lumin., 2009, 129, 874-878. https://doi.org/10.1016/j.jlumin.2009.03.027
[12] Shanmugam N., Dhanaraj K., Viruthagiri G., Balamurugan K., Deivam K., Synthesis and characterization of surfactant-assisted Mn2+ doped ZnO nanocrystals, Arabian J. Chem., 2016, 9, 758-764. https://doi.org/10.1016/j.arabjc.2011.08.016
[13] Carnes C.L., Klabunde K.J., Synthesis, Isolation, and Chemical Reactivity Studies of Nano-crystalline Zinc Oxide, Langmuir., 2000,16, 3764–3772. https://pubs.acs.org/doi/abs/10.1021/la991498p
[14] Sharma N., Jandaik S., Kumar S., Synergistic activity of doped zinc oxide nanoparticles with antibiotics: ciprofloxacin, ampicillin, fluconazole and amphotericin B against pathogenic microorganisms, An Acad Bras Cienc., 2016, 88, 1689-1698. http://dx.doi.org/10.1590/0001-3765201620150713.
[15] Khan S.A., Noreen F., Kanwal S., Hussain G., Comparative synthesis, characterization of Cu-doped ZnO nanoparticles and their antioxidant, antibacterial, antifungal and photocatalytic dye degradation activities, Dig. J. Nanomater. Biostruct., 2017, 12, 877 – 889.
[16] Awwad M., Albiss B., Ahmad L., Green synthesis, characterization and optical properties of zinc oxide nanosheets using Olea Europea leaf extract, Adv. Mater. Lett., 2014, 5, 520-524.
[17] Hudlikar M., Joglekar S., Dhaygude M., Kodama K., Latex-mediated synthesis of ZnS nanoparticles: green synthesis approach, J. Nanopart. Res., 2012, 14, 865-70. https://link.springer.com/article/10.1007/s11051-012-0865-x
[18] Singhal G., Bhavesh R., Kasariya K., Sharma A.R, Singh R.P., Biosynthesis of silver nanoparticles using Ocimum sanctum (Tulsi) leaf extract and screening its antimicrobial activity, J. Nanopart. Res., 2011,13, 2981–2988. https://link.springer.com/article/10.1007/s11051-010-0193-y
[19] Yedurkar S., Maurya C., Mahanwar P., Biosynthesis of Zinc Oxide Nanoparticles Using Ixora Coccinea Leaf Extract—A Green Approach, Open J. Synth. Theory Appl., 2016, 5, 1-14. 10.4236/ojsta.2016.51001
[20] Alagumuthu G., Kirubha R., Green synthesis of silver nanoparticles using Cissusquadrangularis plant extract and their antibacterial activity, Int. J. Nanomater. Biostru., 2012, 2, 30–33.
[21] Mason C., Vivekanandhan S., Misra M., Mohanty A.K., Switchgrass (Panicumvirgatum) extract mediated green synthesis of silver nanoparticles, World J. Nano Sci. Eng., 2012,2, 47–52.
[22] Kundu P., Barik S., Sarkar, K., Bose A., Baral R., Laskar S., Chemical investigation of neem leaf glycoprotein used as immunoprophylactic agent for tumor growth restriction, Int. J. Pharm. Sci., 2015, 7, 195-199.
[23] Soni H., Mishra K ., Sharma S., Singhai A. K., Characterization of Azadirachtin from ethanolic extract of leaves of Azadirachtaindica, J. Pharm. Res., 2012, 5, 199-201.
[24] Maurya Y.C., Mahanwar P., Biosynthesis of Zinc Oxide Nanoparticles Using IxoraCoccinea Leaf Extract—A Green Approach, Open J. Synth. Theory Appl., 2016, 5,1-14. 10.4236/ojsta.2016.51001
[25] Abbasi A., Gharib M., Najafi M., Preparation of ZnO Nanocrystals with Desired Morphology from Coordination Polymers through a Solid-state Decomposition Route, J. Sci., Islamic Repub. Iran., 2016, 27, 217 – 221.
[26] Kulkarni S.S., Mahavidyalaya S., Optical and Structural Properties of Zinc Oxide Nanoparticles, Int. J. Adv. Res. Phys., 2015, 2, 14-18.
[27] Hong R., Li J., Chen L., Liu D., Li H., Zheng Y., Ding J., Synthesis, surface modification and photocatalytic property of ZnO nanoparticles, Powder. Technol, 2009, 189, 426–432. http://dx.doi.org/10.1016/j.powtec.2008.07.004
[28] Thirumavalavan M., Huang K. L., Lee J. F., Preparation and morphology studies of nano zinc oxide obtained using native and modified chitosans, Materials, 2013, 6, 4198–4212.